

Shared-use lane assignment and signal timing optimization at intersections with waiting area

ZHOU Yaping, ZHOU Qiaoqi, ZHUANG Hongbin, ZHENG Jianxin, ZHANG Yanyan
(School of Management, University of Science and Technology of China, Hefei 230026, China)

Abstract: Based on the shared-use lane control method of intersection with left-turn waiting area configuration, a comprehensive optimization model with lane allocation and signal timing optimization was proposed to obtain the optimal design of shared-use lane assignment and signal timing, which is a mixed integer nonlinear programming model. A feasible directions method was hence introduced to solve the mixed integer non-linear programming. The research result shows that the improved control method and optimization model effectively improve the traffic efficiency of the intersections and minimize the average delay of the intersection. The comparison between the shared-use configuration with waiting area and the conventional configuration was presented and the result verifies that the former shows better performance than the latter. Besides, the sensitivities of the optimized average delay were investigated, which include the length of waiting area and the arrival rates. The optimal results proposed by the integrated model may enrich the design of signalized intersections with waiting area.

Key words: waiting area; shared-use lane; lane assignment; signal timing; delay estimation

CLC number: U491.23 **Document code:** A doi:10.3969/j.issn.0253-2778.2020.02.017

Citation: ZHOU Yaping, ZHOU Qiaoqi, ZHUANG Hongbin, et al. Shared-use lane assignment and signal timing optimization at intersections with waiting area [J]. Journal of University of Science and Technology of China, 2020, 50(2): 220-235.

周亚平,周巧琪,庄宏斌,等. 基于待转区的车道共用交叉口车道分配和信号配时优化研究[J]. 中国科学技术大学学报, 2020, 50(2): 220-235.

基于待转区的车道共用交叉口车道分配和信号配时优化研究

周亚平,周巧琪,庄宏斌,郑建新,张妍妍

(中国科学技术大学管理学院,安徽合肥 230026)

摘要: 针对结合左转弯待转区的车道共用控制方式,建立了一种以车道分配和信号配时最优为目标的综合优化模型,即混合整数非线性规划模型,并运用可行方向方法优化配时参数. 结果发现,改进的控制方式和优化模型有效提高了交叉口的通行效率,且使交叉口平均延误得以最小化. 此外,不仅对待行区结合共用车道的改进交叉口设计和传统的交叉口配置进行了比较和分析,验证了前者比后者有更好的运行效果,还对改进方案的平均延误、待转区长度和到达率进行灵敏度分析. 综合优化模型的最优结果为带有待行区的信号交叉口设计的拓展研究提供了有益的参考.

Received: 2018-12-29; **Revised:** 2019-04-09

Foundation item: Supported by Key Project of Soft Science Foundation in Anhui Province of China (1607a0202074).

Biography: ZHOU Yaping (corresponding author), male, born in 1963, PhD/associate Prof. Research field: Management science and engineering. E-mail: zhouyp@ustc.edu.cn

关键词：待转区；共用车道；车道分配；信号配时；延误估计

0 Introduction

Nowadays in China, left-turn waiting area is commonly established in urban signalized intersections with the purpose of discharging more vehicles in the green interval. It was first introduced in Road Traffic Signs and Markings (GB 5768-1999) by Ministry of Transport of the People's Republic of China^[1] and later formally adopted in the version (GB 5768. 3-2009) by the General Administration of Quality Supervision, Inspection and Quarantine of the People's Republic of China in 2009^[2]. The left-turn waiting area is an extension of the dedicated left turn lane entering the intersection, and there are data of related research shows the proof of operational efficiency and safety performance of the left-turn waiting strategy^[3-5]. Jiang et al. focused on the safety performance of the signalized intersections with left-turn waiting area by adopting the traffic conflict technique and compared the discrepancy of conflict types between intersections with left-turn waiting area and without. Results demonstrate that the left-turn volume and driving outside the left-turn waiting area significantly increase the severities of traffic conflicts at the left-turn waiting area^[5]. And the other hand is that the left-turn waiting area layout can effectively reduce the possibility of left-handed vehicle stranding and queuing overflow^[6]. In addition to emphasizing the effect of left-turn waiting area to the operational efficiency, Ma et al. discussed the impact of left-turn waiting areas on operation of signalized intersection from the perspective of motor vehicle efficiency, which chose average control delay of approach as critical criterion. And the layout of setting left-turn waiting area can improve the left-turn traffic flow capacity^[7]. Sun et al. studied the effectiveness of left-turn waiting area implementation by using micro-simulation VISSIM. The simulation results of different types

of left-turn waiting area show that using left-turn waiting area decrease total delay of the intersection^[8]. And there are only a few literature focusing on the impact of the left-turn waiting area on vehicle emissions of signalized intersections with left-turn waiting area^[9].

Fig. 1 presents a typical signalized intersection with a left-turn waiting area in Hefei, China. The geometric configuration is operated in protected left-turn phase since left-turning movements may adversely affect the safety and efficiency of intersections. However, turning flow with fluctuating arrival rates in protected phase may lead to the capacity reduction and delay increase. To handle the imbalance traffic movements of through flow and left-turns, a novel approach to utilize left-turn waiting area in protected phase is proposed by incorporating a shared-use lane geometric design.

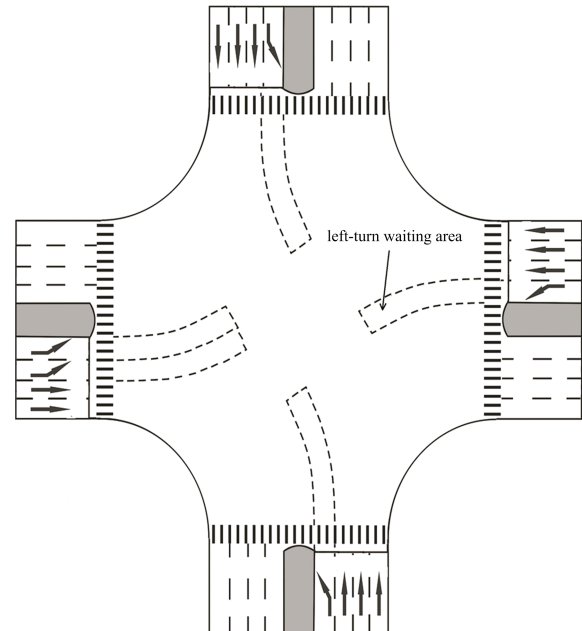


Fig. 1 Current intersection with left-turn waiting area

As is presented in Fig. 2, the four-phase control based on dual-ring structure is adopted with two fully protected left-turn phases. Exclusive left-turn phase, which provides for simultaneous movement of opposing left turns,

follows through phase in each signal cycle. The exclusive left-turns should wait in the area until the through vehicles discharge and protected left-turn phase starts. Hence the potential of an intersection in current configuration is limited.

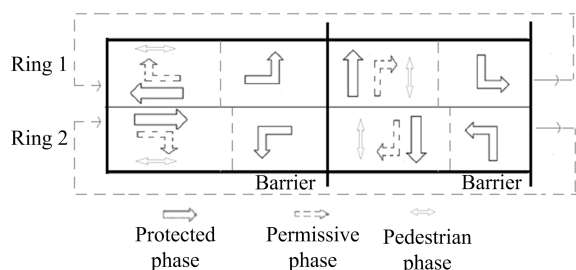


Fig. 2 Signal phasing

As is shown in Fig. 3, the geometric configuration is improved by turning an exclusive left-turn lane or an exclusive through lane into shared-use lane. Meanwhile, several modifications and restrictions are adopted including: (a) isolating and narrowing the waiting area to minimize the conflict between through and left-turn vehicle flow; (b) moving the area to the left for safety concern if the median strip is wide enough; (c) left-turns are required to enter the waiting area to prevent the blockage to the following through vehicles in shared-use lane during the through phase; (d) besides, vehicles are not supposed to change lanes freely as they get close to the stop lane.

When vehicles approach the intersection, for the shared-use configuration, the warrant to enter the waiting area starts from the beginning of the through phase and ends after the left-turn phase, whereas no restriction for turning vehicles exists in the left-turn pocket. In other words, left-turn vehicles enter into the waiting area while through vehicles pass through the intersection during the through phase. That means no vehicles are supposed to remain in left-turn waiting area when the following through phase begins. Left-turn vehicles in the waiting area won't block through vehicles' way, since the waiting area is moved forward and left. However, if the queue length of left-turns exceeds the waiting area length, the

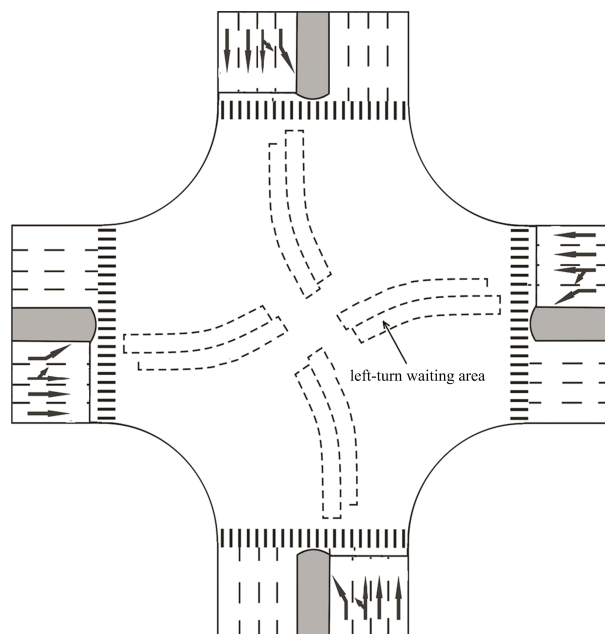


Fig. 3 Improved geometric design with shared-use lane

through vehicles will get stuck. The failure follows a probabilistic mechanism that can be captured in some formulas by considering the length of waiting area, the green time and lane assignment; hence the capacity of the shared-use lane is expected to be calculated. By turning the exclusive left-lane into shared-use lane and utilizing the waiting area, intersections show better performance than the conventional configuration in most cases.

Previous works mainly focused on the capacity of shared-use configuration compared to the exclusive operation in different conditions, such as the existence of left-turn bay or channelization^[10], the permissive or protected signal operation^[11], the gap acceptance in permissive configuration^[12] and so on. Lin^[13], Easa and Ali^[14], Zhang and Tong^[15] focused on the left turn bay and attempted to establish the relationship among the capacity, the traffic delay, signal timing and geometric conditions. Chang and Sun^[16], Zhao et al.^[17] and Zhu et al.^[18] investigated the safety concern on overflow and blockage between the left lane and adjacent lane. Kikuci and Kronpasert^[19] and Qi et al.^[20] discussed the estimation and optimization of the left turn length. As for the signal timing in literature, it mainly includes the pre-timed signal

control, semi-actuated signal control, and fully actuated signal control. Although the pre-timed signal control is focused in the paper, the researchers have applied various methods for signal timing. The general signal timing methods were first presented in the stage-based method and later developed into the group-based method^[21-23]. Different signal timing optimization algorithms focusing on various traffic contexts were thereafter introduced by researchers. These algorithms mainly include genetic algorithm^[24-26] which is used to solve the signal timing optimization model for single-point intersections^[27] and multi-intersection signal control schemes^[28], fuzzy optimization algorithm^[29], dynamic programming algorithm^[30-31], bi-level programming model of signal timing optimization with the Gauss-Seidel iterative solution algorithm^[32], platoon-based traffic signal timing algorithm^[33], maximal progression possibility operation algorithm^[34], multi-objective joint optimization converted to a single-objective function solution algorithm^[35] and urban traffic control system algorithm based on deep reinforcement learning (DRL). The latter two algorithms are relatively recent optimization algorithms, especially the urban traffic signal control algorithm based on DRL which is an urban traffic control system based on deep reinforcement learning (DRL) presented to solve traffic congestion and improve traffic flow, and the method shows more promising results than other methods based on DRL after simulation experiments and comparative analysis, which verify that the method can adapt to the complex dynamically changing environment^[36]. The signal timing combined with the optimal lane assignment is observed and proposed in an integrated model^[37-39]. They present a lane-based optimization method for the integrated design of lane markings and signal settings for isolated junctions and convert the optimization problems into Binary-Mix-Integer-Linear-Programs. However, the traffic behavior in the shared-use lane with

waiting area is much complicated than the conventional geometric configuration, because the de facto lanes utilized by through or turning vehicles should be recalculated by the probability theory^[40-42].

In this work, a feasible directions method to solve the shared lane configuration optimization was proposed. The lane assignment and signal timing optimization is integrated to investigate the optimal design of lane-use and signal-phase control in the new configuration. The optimization eliminates the potential inferior performance, despite the fact that the disadvantage only exists in some extreme situation. The results of the integrated model for optimal design of the shared-use lane assignment and signal timing optimization show significant improvement in minimizing average delay and increasing capacity of the intersection.

The rest of the paper is organized as follows. Constraints, notations and processing steps are first described in the subsequent sections. Next, the algorithm is presented and numerical examples are discussed in detail. The final section concludes the paper and suggests the direction for future work.

1 Constraints for shared-use lane assignment

The purpose of the new geometric configuration is to release more through (or left-turn) vehicles without compromising the efficiency of left-turn (or through) vehicles. For an isolated intersection, it is assumed that the arriving vehicles from the upstream of an approach will choose the corresponding lane with shortest queue length. Hence, the queue in each lane will be roughly equal on average in general. Fig. 3 presents common configuration with the waiting area in front of the shared-use lane. The shared-use lane assignment, also known as shared-use lane designation, is incorporated in this section.

1.1 Label transition of arms

The configuration is basically operated in the at-grade intersection with four arms and the arms are marked by using clockwise rotation. To depict the label transition relationship among the approaches, three functions are defined below.

$$m_1(i) = \text{mod}(i + 1, 4) + 4\{1 - \text{sgn}[\text{mod}(i + 1, 4)]\} \quad (1)$$

$$m_2(i) = \text{mod}(i + 2, 4) + 4\{1 - \text{sgn}[\text{mod}(i + 2, 4)]\} \quad (2)$$

$$m_3(i) = \text{mod}(i + 3, 4) + 4\{1 - \text{sgn}[\text{mod}(i + 3, 4)]\} \quad (3)$$

where $\text{sgn}(\cdot)$ is the sign function, $\text{sgn}(x) = 1$ if $x > 0$, $\text{sgn}(x) = 0$ if $x = 0$, and $\text{sgn}(x) = -1$ if $x < 0$. $\text{mod}(\cdot)$ is a modulo operation to find the remainder of division of one number by another. Arm $m_1(i)$ is the arm located on the left side of arm i , whereas arm $m_2(i)$ is the one located at the opposite direction of arm i and similarly, arm $m_3(i)$ is the one located at the right side of arm i , where $i = 1, 2, 3, 4$. The first part in equations reflects the label transition and the second part is to prevent zeros in some modulo operation. Besides, the approach in one arm shares the same label with the corresponding arm.

1.2 Shared-use lane assignment constraint

Let $\gamma(i, j, k)$ be the binary variable for traffic movement from lane k of approach i flows into arm j , where $i, j = 1, 2, 3, 4$, $j \neq i$, $k = 1, 2, \dots, a_i$ and a_i is the number of lanes in arm i . $\gamma(i, j, k) = 1$ if the movement is permitted and $\gamma(i, j, k) = 0$ if prohibited. Lanes in an approach are numbered from median strip to nearside, namely k is marked from inner to outer on each arm.

For each approach, inspired by Ref. [38], the following constraints should be satisfied to prevent the conflict between through vehicles and turning vehicles. If left-turn vehicles are permitted to enter a certain lane, regardless of exclusive or shared-use operation, all lanes on the left should be the exclusive left-turn ones, which is equivalent to

$$\gamma(i, m_1(i), k) \leq \gamma(i, m_1(i), k - 1) \quad (4)$$

where

$$i = 1, 2, 3, 4; k = 2, 3, \dots, a_i.$$

Similarly, if right-turn vehicles are permitted to enter a certain lane, regardless of exclusive or shared-use operation, all lanes on the right should be the exclusive right-turn ones, which is equivalent to

$$\gamma(i, m_3(i), k - 1) \leq \gamma(i, m_3(i), k)$$

where

$$i = 1, 2, 3, 4; k = 2, 3, \dots, a_i.$$

Obviously, in one approach, there should not be more than two shared-use lanes; otherwise the conflicts among different movements may happen. The constraint hence is given by

$$\sum_{k=1}^{a_i} (\gamma(i, m_1(i), k) + \gamma(i, m_2(i), k) + \gamma(i, m_3(i), k)) \leq a_i + 2 \quad (6)$$

Besides, no lane will be left unused, which means

$$\sum_{j=1, j \neq i}^4 \gamma(i, j, k) \geq 1 \quad (7)$$

where

$$i = 1, 2, 3, 4; k = 2, 3, \dots, a_i.$$

1.3 Lane constraint for approaches and exits

Since the total lanes in an arm is subjected by the local geometric condition, the number of lanes in total is a constant, regardless the lane allocation for approach and exit flow. Therefore, the constraint is given by

$$a_i + e_i = L_i \quad (8)$$

where a_i is the number of lanes of approach i , e_i is the number of lanes of exit i , and $L_i =$ the total lane in one arm i .

1.4 Matching saturation flow rate

When traffic movements flow across an intersection into the exits, it is critical to make sure that the saturation flow rates of exits are not less than the total saturation flow rate required by the traffic movements in each phase; otherwise, the vehicles will accumulate in the intersection which may result in congestion. Let μ_{ik}^a be the saturation flow rate of lane k of approach i , μ_{ik}^e be the saturation flow rate of lane of exit i , the

equation of relationship between μ_{ik}^a and μ_{ik}^e can be expressed as following ,

$$\sum_{i=1, i \neq j}^4 \sum_{k=1}^{a_i} \gamma(i, j, k) \mu_{ik}^a \delta(i, j, t) \leq \sum_{k=1}^{e_j} \mu_{jk}^e \quad (9)$$

where $i, j = 1, 2, 3, 4$; $\delta(i, j, t)$ is the binary variable of right-of-way of movement from approach i to exit j in time t and $0 \leq t \leq C$. $\delta(i, j, t) = 1$ indicates that the movement is allowed to flow into exit and is forbidden if $\delta(i, j, t) = 0$.

Fig. 4 illustrates the intersection structure is presented below. The lane assignment is predetermined to help the readers better understanding the configuration. The movement $(i, m_1(i), 1)$ represents the flow from lane 1 of arm i moving toward arm $m_1(i)$. Therefore, $\gamma(i, m_1(i), 1)$ shall denote the lane assignment and $\delta(i, j, t)$ represent the right-of-way of the movement $(i, m_1(i), 1)$.

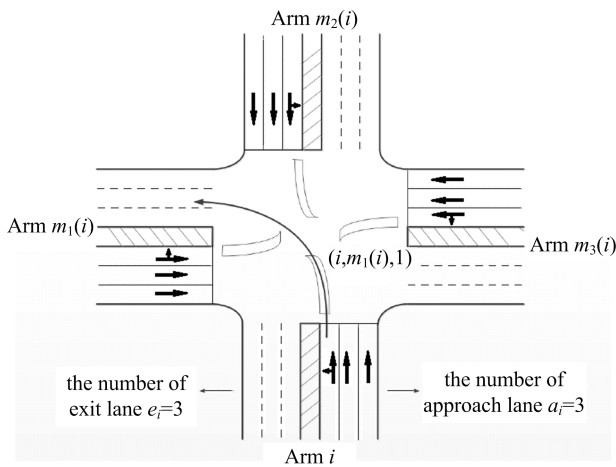


Fig. 4 An example of intersection structure, lane assignment, and notations corresponding to a left-turn movement

2 Approach capacity of shared-use configuration with waiting area

The paper aims to minimize the average delay of vehicles in intersections with waiting area. Hence, the capacity of shared-use lane with waiting area should be clarified before the optimization. In the following, the paper will focus on the shared-use pattern that through vehicles share a lane with left-turn vehicles.

2.1 Relevant parameters that determine the capacity of shared-use lane

The waiting area is operated in front of the shared-use lane; hence the length of waiting area has to be considered in the calculation of capacity. Besides, the length of green phase will affect the actual number of vehicles discharged in one cycle; therefore the signal timing should be incorporated in the capacity analysis. Since the number of vehicles discharged in exclusive through or left-turn lane in one cycle is the same as that of the conventional design, the number of vehicles discharged in shared-use lane is taken into consideration.

It is important to realize that if the length of waiting area is too short, through vehicles may be blocked by the excessive left-turn vehicles, which will result in traffic jam. However, the possibility that blockage occurs is determined by the relevant parameters. In this section, the signal phase will be considered as a parameter rather than variable to investigate the capacity.

In the follows, subscripts f and l indicate through and left-turn vehicle respectively, whereas right-turns are neglected in the paper. N is the maximum number of vehicles discharged in shared-use lane during the through phase regardless of vehicle type, and M is the maximum number of vehicles discharged in shared-use lane during the left-turn phase regardless of vehicle type. B shall denote the length of waiting area, which represents the maximum number of vehicles that can be accommodated in the waiting area. The probability of vehicles being through or left-turn in the shared lane, which is denoted by p_f and p_l respectively, can be determined by the proportion of left-turn and through volume in the approach. $prob_i$ shall denote the probability that i vehicles, whether through or left-turn, be discharged in the shared-lane. The capacity of shared lane is deduced by the comparison of relevant parameters B , M and N , which is presented below. The different conditions are categorized into two cases for through vehicles and three cases for left-turns in the shared lane.

2.2 Through vehicles discharged in shared lane

To utilize the left-turn waiting area in the share lane, it assume that the left-turn phase follows through phase, as is presented in Fig. 2. Thus the number of through vehicles discharged is correlated to the length of waiting area B and the maximum number of vehicles discharged at the saturation flow rate during through phase, denoted by N . The situations are categorized in the following two cases:

If $B \geq N$, the number of through vehicles discharged shall follow a binomial distribution and the probability that i through vehicles discharged in case $B \geq N$ can be summarized as

$$\text{prob}_i = C_N^i p_f^i p_l^{N-i} \quad (10)$$

where $i = 1, 2, \dots, N$, C_N^i equals to $\binom{N}{i} =$

$\frac{N!}{i!(N-i)!}$ and p_f^i represents the probability that i through vehicles are discharged and p_l^{N-i} is the probability that $N - i$ left-turn vehicles are discharged.

If $B < N$, since waiting area is inadequate to accommodate all the through vehicles, the blockage may happen in some situations. The probability that i through vehicles discharged in case $B < N$ in one cycle is given by

$$\text{prob}_i = \begin{cases} C_{B+i}^i p_f^i p_l^{B+1}, & \text{if } i \leq N - B - 1; \\ C_N^i p_f^i p_l^{N-i}, & \text{if } N - B \leq i \leq N \end{cases} \quad (11)$$

By summarizing Case 1 and Case 2, the expectation of through vehicles discharged in one signal cycle is

$$E^f = \begin{cases} \sum_{i=0}^{N-B-1} C_{B+i}^i p_f^i p_l^{B+1} i + \sum_{i=N-B}^N C_N^i p_f^i p_l^{N-i} i, & \text{if } B < N; \\ \sum_{i=0}^N C_N^i p_f^i p_l^{N-i} i, & \text{if } B \geq N \end{cases} \quad (12)$$

A detailed formula derivation of Eqs. (10) ~ (12) can be found and seen in Ref. [30], and it wouldn't be presented in detail in the paper.

2.3 Left-turn vehicles discharged in shared lane

Because left-turn phase follows through

phase, the number of left-turns discharged in the shared-lane is correlated to B , M and N , and the discussion is categorized into three cases by the comparison among B , M and N .

If $M \leq \min\{B, N\}$, the probability that i left turn vehicles discharged in the case of $M \leq \min\{B, N\}$ is

$$\text{prob}_i = \begin{cases} \sum_{j=0}^i C_N^j p_l^j p_f^{N-j+1}, & \text{if } i < M; \\ \sum_{j=0}^i C_N^j p_l^j p_f^{N-j}, & \text{if } i = M \end{cases} \quad (13)$$

where j is the number of left-turn vehicles entering the waiting area during through phase.

If $B < \min\{M, N\}$, the probability that i left turn vehicles discharged in the case of $B < \min\{M, N\}$ is

$$\text{prob}_i = \begin{cases} \sum_{j=0}^i C_N^j p_l^j p_f^{N-j+1}, & \text{if } i \leq B; \\ \sum_{j=0}^{B-1} C_N^j p_l^j p_f^{N-j+1} + \sum_{z=B}^N \sum_{k=0}^{N-z} C_{z-1}^{B-1} p_l^i p_f^{z-B+k+1}, & \\ \quad \text{if } B < i < M; \\ \sum_{j=0}^{B-1} C_N^j p_l^j p_f^{N-j} + \sum_{z=B}^N \sum_{k=0}^{N-z} C_{z-1}^{B-1} p_l^i p_f^{z-B+k}, & \\ \quad \text{if } i = M \end{cases} \quad (4)$$

where vehicle z is the last left-turn one that can enter the waiting area and k is the number of continuous through vehicles after vehicle z .

If $N < M$ and $N \leq B$, the probability that i left turn vehicles discharged subjected to $N < M$ and $N \leq B$ is

$$\text{prob}_i = \begin{cases} \sum_{j=0}^i C_N^j p_l^j p_f^{N-j+1}, & \text{if } i \leq N; \\ \sum_{j=0}^N C_N^j p_l^j p_f^{N-j+1}, & \text{if } N < i < M; \\ \sum_{j=0}^N C_N^j p_l^j p_f^{N-j}, & \text{if } i = M \end{cases} \quad (15)$$

By summarizing Cases 4, 5 and 6, the expectation of left-turns discharged in one signal cycle is given by

$$E^l = \sum_{i=0}^M \text{prob}_i i \quad (16)$$

with prob_i determined by Eqs. (13)~(15) in three different cases. A detailed formula derivation of Eqs. (13)~(16) can be seen in Ref. [30] for better understanding.

3 Relationship between the capacity of lane groups and signal timing

In the capacity analysis above, N and M are integers, which are proportional to the green length $g_{i,m_2(i)}$ and $g_{i,m_1(i)}$. Without loss of generality, let the lane k of arm i be the shared-use lane, the number of vehicles that can be discharged in the saturation flow during the through phase is $\hat{N}_{ik} = g_{i,m_2(i)} \mu_{ik}^a$, where $i = 1, 2, 3, 4$, $k = 1, 2, \dots, a_i$. Similarly, the number of vehicles that can be discharged in the saturation flow during the left-turn phase is $\hat{M}_{ik} = g_{i,m_1(i)} \mu_{ik}^a$. It is obvious that \hat{N}_{ik} and \hat{M}_{ik} are continuous variables, which cannot be used in (10) to (16), because integers are required in the calculation.

The number of vehicles discharged in the saturation flow during the through phase, however, is a stochastic variable and the value can be either $N_{ik} = \lfloor \hat{N}_{ik} \rfloor$ or $N_{ik} = \lfloor \hat{N}_{ik} \rfloor + 1$. The probability is $\text{prob}\{N_{ik} = \lfloor \hat{N}_{ik} \rfloor\} = \lfloor \hat{N}_{ik} \rfloor + 1 - \hat{N}_{ik}$ or $\text{prob}\{N_{ik} = \lfloor \hat{N}_{ik} \rfloor + 1\} = \hat{N}_{ik} - \lfloor \hat{N}_{ik} \rfloor$, which are concisely denoted by \underline{P}_{ik}^N and \overline{P}_{ik}^N respectively.

Similarly, the number of vehicles discharged in saturation flow during the left-turn phase is a stochastic variable and the value can be $M_{ik} = \lfloor \hat{M}_{ik} \rfloor$ or $M_{ik} = \lfloor \hat{M}_{ik} \rfloor + 1$. The probability is $\text{prob}\{M_{ik} = \lfloor \hat{M}_{ik} \rfloor\} = \lfloor \hat{M}_{ik} \rfloor + 1 - \hat{M}_{ik}$ or

$$\text{prob}\{M_{ik} = \lfloor \hat{M}_{ik} \rfloor + 1\} = \hat{M}_{ik} - \lfloor \hat{M}_{ik} \rfloor,$$

which are concisely denoted by \underline{P}_{ik}^M and \overline{P}_{ik}^M respectively.

Based on the analysis above, it is easy to prove that the expectation of stochastic variable N_{ik} and M_{ik} are $E(N_{ik}) = \hat{N}_{ik}$ and $E(M_{ik}) = \hat{M}_{ik}$ respectively. For example, if $g = 14$ s and $\mu = 0.46$ veh/s, then the accurate number of vehicles discharged is 6.44, which cannot be used in Eqs. (10)~(16). However based on the assumptions

above, the number can be considered to be 7 with the probability 0.44 and 6 with the probability 0.56. Hence the number of vehicles discharged is 6 or 7, which can be used in Eqs. (10)~(16). To obtain the expectation of through and left-turn vehicles, the following steps are presented.

Step 1 Let $N = \lfloor \hat{N}_{ik} \rfloor = \lfloor \mu_{ik}^a g_{im_2(i)} \rfloor$ and $M = \lfloor \hat{M}_{ik} \rfloor = \lfloor \mu_{ik}^a g_{im_1(i)} \rfloor$, and put N , M , B into Eqs. (10)~(16), hence E^f and E^l with lower value N and M are shown, and $E_{ik}^f(\underline{N}, \underline{M}) = E^f$ and $E_{ik}^l(\underline{N}, \underline{M}) = E^l$ are defined in this case.

Step 2 Let $N = \lfloor \hat{N}_{ik} \rfloor + 1$ and $M = \lfloor \hat{M}_{ik} \rfloor$, and put N , M , B into Eqs. (10)~(16), hence E^f and E^l with higher value N and lower M are shown, and $E_{ik}^f(\overline{N}, \underline{M}) = E^f$ and $E_{ik}^l(\overline{N}, \underline{M}) = E^l$ are defined in this case.

Step 3 Let $N = \lfloor \hat{N}_{ik} \rfloor$ and $M = \lfloor \hat{M}_{ik} \rfloor + 1$, and put N , M , B into Eqs. (10)~(16), hence E^f and E^l with lower N and higher M are shown, and $E_{ik}^f(\underline{N}, \overline{M}) = E^f$ and $E_{ik}^l(\underline{N}, \overline{M}) = E^l$ are defined in this case.

Step 4 Let $N = \lfloor \hat{N}_{ik} \rfloor + 1$ and $M = \lfloor \hat{M}_{ik} \rfloor + 1$, and put N , M , B into Eqs. (10)~(16), hence E^f and E^l with both higher value N and M are shown, and $E_{ik}^f(\overline{N}, \overline{M}) = E^f$ and $E_{ik}^l(\overline{N}, \overline{M}) = E^l$ are defined in this case.

Step 5 With the probability \underline{P}_{ik}^N , \overline{P}_{ik}^N , \underline{P}_{ik}^M , \overline{P}_{ik}^M , the equations can be expressed as following,

$$\text{prob}\{N = \lfloor \hat{N}_{ik} \rfloor, M = \lfloor \hat{M}_{ik} \rfloor\} = \underline{P}_{ik}^N \underline{P}_{ik}^M \quad (17)$$

$$\text{prob}\{N = \lfloor \hat{N}_{ik} \rfloor + 1, M = \lfloor \hat{M}_{ik} \rfloor\} = \overline{P}_{ik}^N \underline{P}_{ik}^M \quad (18)$$

$$\text{prob}\{N = \lfloor \hat{N}_{ik} \rfloor, M = \lfloor \hat{M}_{ik} \rfloor + 1\} = \underline{P}_{ik}^N \overline{P}_{ik}^M \quad (19)$$

$$\text{prob}\{N = \lfloor \hat{N}_{ik} \rfloor + 1, M = \lfloor \hat{M}_{ik} \rfloor + 1\} = \overline{P}_{ik}^N \overline{P}_{ik}^M \quad (20)$$

Hence the expectation of through vehicles discharged in shared lane is hence given by

$$\begin{aligned} \hat{E}_{ik}^f &= \underline{P}_{ik}^N \underline{P}_{ik}^M E_{ik}^f(\underline{N}, \underline{M}) + \overline{P}_{ik}^N \underline{P}_{ik}^M E_{ik}^f(\overline{N}, \underline{M}) + \\ &\quad \underline{P}_{ik}^N \overline{P}_{ik}^M E_{ik}^f(\underline{N}, \overline{M}) + \overline{P}_{ik}^N \overline{P}_{ik}^M E_{ik}^f(\overline{N}, \overline{M}) \quad (21) \end{aligned}$$

Similarly, the expectation of left-turn vehicles discharged in shared lane equals

$$\hat{E}_{ik}^l = \underline{P}_{ik}^N \underline{P}_{ik}^M E_{ik}^l(\underline{N}, \underline{M}) + \overline{P}_{ik}^N \underline{P}_{ik}^M E_{ik}^l(\overline{N}, \underline{M}) +$$

$$\overline{P}_{ik}^N \overline{P}_{ik}^M E_{ik}^l(N, \overline{M}) + \overline{P}_{ik}^N \overline{P}_{ik}^M E_{ik}^l(\overline{N}, \overline{M}) \quad (22)$$

Step 6 By using Eqs. (21) and (22), the number of through and left-turn vehicles discharged in the shared lane are obtained. Therefore, the capacity of through lane groups is modified, which is given by

$$\mu_{i,m_2(i)} = \sum_{h=k+1}^{a_i} \mu_{ih}^a + \frac{\widehat{E}_{ik}^f}{g_f} \quad (23)$$

And the capacity of left-turn lane groups is given by

$$\mu_{i,m_1(i)} = \sum_{h=1}^{k-1} \mu_{ih}^a + \frac{\widehat{E}_{ik}^l}{g_l} \quad (24)$$

4 Objective functions and average delay estimation

The Webster's delay formula^[43] is presented to calculate the average delay that vehicles experienced in intersections. The saturation flow rate of through lanes and left-turn lanes, however, are replaced by using (23) and (24) respectively. The average delay of vehicles from arm i to arm j is given by

$$d(i, j) = \frac{r_{ij}^2}{2C[1 - (\lambda_{ij}/\mu_{ij})]} + \frac{R_{ij}^2}{2\lambda_{ij}(1 - R_{ij})} - 0.65 \left(\frac{C}{\lambda_{ij}^2} \right)^{1/3} R^{(2+5g_{ij}/C)} \quad (25)$$

where g_{ij} = green length that allows movement from approach i moving into exit j . r_{ij} = effective red time from approach i to exit j and $r_{ij} = C - g_{ij}$, $i = 1, 2, 3, 4$, $j = 1, 2, 3, 4$. λ_i = average arrival rate of traffic flow in approach i . λ_{ij} = average arrival rate of movement from approach i to exit j , where $\lambda_{ij} = \lambda_i \alpha_{ij}$ and α_{ij} is the proportion of vehicles in approach i moving into exit j . R_{ij} = degree of saturation, where $R_{ij} = \lambda_{ij}/(\mu_{ij}g_{ij}/C)$ and μ_{ij} is obtained from (23) or (24). C = cycle length. Hence the average delay of an intersection is

$$aveD = \sum_{i=1}^4 \lambda_i \sum_{j=1}^4 \alpha_{ij} d(i, j) / \sum_{i=1}^4 \lambda_i \quad (26)$$

where α_{ij} is the proportion of vehicle from arm i to arm j .

Therefore, the objective function of the optimal lane assignment and signal timing in the new configuration is to minimize (26). The

constraint (4) to (9) ensure vehicles can orderly and safely discharge from intersections. The variables are the green length g_{ij} , the binary variables $\gamma(i, j, k)$ and $\delta(i, j, t)$. The parameters include the saturation flow rate μ_{ik}^a and μ_{ik}^e , the number of lanes in approach and exit a_i and e_i , the arrival rate λ_i and turning proportion α_{ij} . The signal cycle is the sum of all phases plus the lost time. By solving the non-linear programming, with the parameters given, the optimal results for the shared-use lane assignment and signal timing are expected to be obtained. The problem is hence converted to a mixed integer non-linear programming and the algorithm is presented below.

The non-linear programming with continuous and binary variables is difficult to be solved since the computational complexity increases exponentially with the number of lane assignment variables. However, the number of lanes in one approach is limited, hence the number of lane assignment can be simplified as the outer loop of the optimization. The general algorithm such as Branch and Bound or Brute-force search can deal with the search of optimal discrete lane assignment plan. In this work, the lane assignment plans are enumerated based on the local geometric configuration. For example, if there are five lanes in an approach, the number of variables $\gamma(i, j, k)$ of the intersection is less than 9^4 since there are only 9 feasible assignments available. Therefore, the problem is converted to a non-linear programming with given value of binary variables.

5 Algorithm for the non-linear programming

A feasible directions method is introduced in this work to solve the non-linear programming. The steps are presented as follows:

Step 1 Let K_m be the total number of shared-use lane assignment plans and $aveD_{\min}$ be minimized average delay with the initial value $aveD_{\min} = +\infty$, and assign $K = 1$.

Step 2 Given the K shared-use lane

assignment, compute the capacity of through or left-turn lane groups by (23) and (24).

Step 3 Define $G = (g_{13}, g_{12}, g_{24}, g_{23}, g_{31}, g_{34}, g_{42}, g_{41})$ as a continuous variable set and the average delay function $aveD(G) = f(G)$, s. t. $g_{13} + g_{34} = g_{12} + g_{31}, g_{24} + g_{41} = g_{23} + g_{42}$.

Step 3.1 Predetermine two sufficient small $\epsilon_1 > 0$ and $\epsilon_2 > 0$, and choose an initial value $G^{(0)} \in R$ while let $k = 0$.

Step 3.2 Judge the state of the constraint indicator set $J(G^{(k)}) = \{j \mid g_j(G^{(k)}) = 0, 1 \leq j \leq l\}$, where l is the number of constraints. If $J(G^{(k)}) \neq \emptyset$, go to Step 3.3. If $J(G^{(k)}) = \emptyset$ and $\|\nabla f(G^{(k)})\|^2 \leq \epsilon_1$, the iteration is halted and the final value $G^{(k)}$ is obtained. If $J(G^{(k)}) = \emptyset$ and $\|\nabla f(G^{(k)})\|^2 > \epsilon_1$, choose the direction vector $d^{(k)} = -\nabla f(G^{(k)})$ and jump to Step 3.5.

Step 3.3 Solve the following linear programming to attain the optimal $d^{(k)}$ and η_k .

$$\begin{aligned} & \min \eta_k \\ \text{s. t. } & \begin{cases} \nabla f(G^{(k)})^T d \leq \eta_k, \\ -\nabla g_j(G^{(k)})^T d \leq \eta_k, j \in J(G^{(k)}), \\ -1 \leq d_i \leq 1, i = 1, 2, \dots, n \end{cases} \end{aligned}$$

where $d = (d_1, d_2, \dots, d_n)$.

Step 3.4 If $|\eta_k| \leq \epsilon_2$ satisfied, the iteration is halted and $G^{(k)}$ is got, else go to next step.

Step 3.5 Solve the following one-dimensional optimization problem $\lambda_k : \min_{0 \leq \lambda \leq \bar{\lambda}} f(G^{(k)} + \lambda d^{(k)})$ where $\bar{\lambda} = \max\{\lambda \mid g_j(G^{(k)} + \lambda d^{(k)}) \geq 0, j = 1, 2, \dots, l\}$.

Step 3.6 Let $G(k+1) = G^{(k)} + \lambda_k d^{(k)}$ and $k := k + 1$, and jump to Step 3.2.

Step 4 Compare $aveD$ with $aveD_{\min}$. If $aveD < aveD_{\min}$, then update $aveD_{\min}$ with $aveD$ and save the optimal lane assignment K^* and signal timing G^* . If else, go to next step.

Step 5 If $K < K_m$, update $K := K + 1$ and jump to Step 2.

Step 6 Save minimal average delay $aveD_{\min}$, optimal lane assignment K^* and signal timing G^* .

6 Numerical examples

An at-grade intersection with four arms is

considered in the paper to demonstrate the advantage of shared-use assignment with waiting area. The optimal shared-use lane assignment and signal timing are presented and the sensitivities of the optimized average delays are thereafter investigated, which include the length of waiting area and arrival rates. The comparison between the proposed shared-use configuration and the conventional configuration is presented below. Both the optimized results of shared-use and conventional configuration are obtained from the algorithm above. The difference lies in the recalculation of the capacity of lane groups, which is relevant to the green length and will hence affect the optimal results. Besides, only exclusive lane assignment is considered in the conventional configuration, otherwise the saturation flow rate of a shared-use lane in permissive signal phase has to be determined, which may not be available in the absence of local condition. The iteration of conventional configuration is therefore less than that of the shared-use configuration since the former has fewer lane assignment plans. The geometric layout and the value of relevant parameters are as follows.

Tab. 1 presents three cases with different input parameters. There are four arms in all three cases and three lanes in Approach 1 or Approach 3, whereas four lanes in Approach 2 or Approach 4. In Case I, each approach has the same length of waiting area and there are four conditions which the length of waiting area is three, four, five and six respectively. And in Case II, each approach has the different length of waiting area, which Condition 1 is high traffic volume and large waiting area while Condition 2 is high traffic volume and small waiting area. In case III, it is discussed that the arrival rate of through and left-turn vehicles in Approach 3 are different from Case I only. Besides, the saturation flow rate is 1650 vehicles per hour per lane, the minimum green time is 10 s, and the lost time in one cycle is 12 s for all cases.

Tab. 1 Geometric layout and the value of relevant parameters

	arm number	number of lanes in the approach	arrival rate	arrival rate	length of waiting area(veh)				length of waiting area(veh)	
			of through vehicles (veh/h)	of left-turn vehicles (veh/h)	four conditions				Condition 1	Condition 2
Case I	1	4	732	600	3	4	5	6		
	2	3	726	390	3	4	5	6		
	3	4	937	575	3	4	5	6		
	4	3	540	360	3	4	5	6		
Case II	1	4	732	600					5	4
	2	3	726	390					4	5
	3	4	937	575					6	3
	4	3	540	360					3	6
Case III	1	4	732	600	3	4	5	6		
	2	3	726	390	3	4	5	6		
	3	4	1350	162	3	4	5	6		
	4	3	540	360	3	4	5	6		

[Note] The “four conditions” indicates that each approach has the same length of waiting area and there are four conditions which the length of waiting area is three, four, five and six respectively.

Tab. 2 gives a comparison of control effects in Case I between the conventional control method and the control method proposed in this paper. For the conventional control, the minimum average delay is 107.5687 s, and the number of vehicles passing through intersection totally are 5385 veh/h. While the average delay of shared-use control proposed in the paper is 61.1061 s when the length of waiting areas of 4 arms are 3, and there are 5654 vehicles passing through intersection per hour. When the length of waiting areas of 4 arms are 4,

the average delay is 55.0284 s, and the total cars passing through intersection are 5836 veh/h. When the length of waiting areas of 4 arms are 5, the average delay is 51.5351 s, and the total cars passing through intersection are 5964 veh/h. When the length of waiting areas of 4 arms are 6, the average delay is 49.4022 s, and the total cars passing through intersection are 6054 veh/h. It finds that the shared-use control method proposed in the paper has obvious advantages compared with the conventional control method.

Tab. 2 Comparisons between the conventional configuration and shared-use configuration with waiting area: Case I

configuration	signal phase(green time/s)								optimized average delay/s	capacity/(veh · h ⁻¹)	
	g_{13}	g_{31}	g_{12}	g_{34}	g_{24}	g_{42}	g_{23}	g_{41}			
conventional	53.3561	58.0274	37.4578	42.129	45.1882	37.3358	52.6658	44.8135	107.5687	5385	
shared-use (length of waiting area)	3	28.1051	32.1159	26.5604	30.5712	29.3576	25.2903	22.2100	18.1427	61.1061	5654
	4	28.2305	31.5258	26.0505	29.3458	30.0213	25.8074	21.693	17.4791	55.0284	5836
	5	27.9180	30.4640	25.1123	27.6583	30.4829	26.2778	21.2226	17.0175	51.5351	5964
	6	27.9604	29.9712	24.6051	26.6158	30.7323	26.5941	20.9063	16.768	49.4022	6054

[Note] The “shared-use (length of waiting area) 3,4,5,6” indicates that each approach has the same length of waiting area and there are four conditions which the length of waiting area is three, four, five and six respectively.

Tab. 3 gives a comparison of control effects in Case II between the conventional control and the control method proposed in this paper. Because the arrival rates of 8 traffic streams in 4 arms in Case I are same as Case II, while the length of waiting areas are different. And the conventional control is uncorrelated to the length of waiting areas, so the optimal lane and green time allocations are identical to those in Case I. For the Condition 1 of Case II, where the length of waiting areas is

positively correlated with the arrival rate of the arm, the minimum average delay is 51.7567 s, and the total cars passing through intersection are 5955 veh/h. And if the length of waiting areas is negatively correlated with the arrival rate in that arm, the minimum average delay of the intersection is 56.1096 s, which is consistent with our intuitive prediction. And there are 5842 vehicles passing through intersection per hour in this condition.

Tab. 3 Comparisons between the conventional configuration and shared-use configuration with waiting area: Case II

configuration	signal phase (green time/s)								optimized average delay/s	capacity/(veh · h ⁻¹)	
	g_{13}	g_{31}	g_{12}	g_{34}	g_{24}	g_{42}	g_{23}	g_{41}			
conventional	53.3561	58.0274	37.4578	42.1290	45.1882	37.3358	52.6658	44.8135	107.5687	5385	
shared-use	Condition 1	27.6493	29.1460	24.4303	25.9270	29.2822	25.9923	21.5080	18.2182	51.7567	5955
	Condition 2	28.7379	33.5432	27.0331	31.8384	30.7526	26.2499	21.2504	16.7477	56.1096	5842

Tab. 4 gives a comparison of control effects in Case III between the conventional control and the control method proposed in this paper. For the conventional control, the minimum average delay is 93.2933 s, and there are 5582 vehicles passing through intersection per hour. While the average delay of shared-use control is 56.0410 s when the length of waiting areas of 4 arms are 3, and the total cars passing through intersection are 5745 veh/h. When the length of waiting areas of 4 arms are 4, the average delay is 50.5402 s, and the total cars passing through intersection are 6063 veh/h. When the length of waiting areas of 4 arms are 5,

the average delay is 47.6802 s, and there are 6308 vehicles passing through intersection per hour. When the length of waiting areas of 4 arms are 6, the average delay is 46.1541 s, and there are 6434 vehicles passing through intersection per hour. Compared with the conventional control method, the shared-use control method proposed in the paper has obvious advantages. In addition, the effect of the control method proposed in the paper to reduce the average delay of the intersection is more obvious with the increase of the length of waiting areas.

Tab. 4 Comparisons between the conventional configuration and shared-use configuration with waiting area: Case III

configuration	signal phase(green time/s)								optimized average delay/s	capacity/(veh · h ⁻¹)	
	g_{13}	g_{31}	g_{12}	g_{34}	g_{24}	g_{42}	g_{23}	g_{41}			
conventional	60.3727	50.2764	33.7820	23.6857	40.7765	33.7034	47.5096	40.4365	93.2933	5582	
shared-use (length of waiting area)	3	29.4878	30.0260	25.7503	26.2885	29.3175	25.2937	22.2066	18.1829	56.0410	5745
	4	32.9776	29.4791	25.1972	21.6987	29.9978	25.8214	21.6790	17.5025	50.5402	6063
	5	35.7172	29.0331	24.5431	17.8590	30.4826	26.2966	21.2038	17.0178	47.6802	6308
	6	36.6162	28.8682	24.0081	16.2601	30.7401	26.6151	20.8852	16.7603	46.1541	6434

[Note] The “shared-use (length of waiting area) 3,4,5,6” indicates that each approach has the same length of waiting area and there are four conditions which the length of waiting area is three, four, five and six respectively.

The optimal lane assignment and markings of three cases are presented in Tab. 5. For the four

conditions of the length of waiting areas in Case I and the two conditions in Case II, the optimal lane

allocation in each approach is consistent, because the lane allocation mainly depends on the arrival rate of through and left-turn vehicles in the approach. The arrival rates of through and left-

turn vehicles of Approach 3 in case III both are different from those of Case I and Case II, so the lane allocation of Case III is also different.

Tab. 5 Optimal lane assignment and markings of cases

configuration	lanes of Arm 1				lanes of Arm 2			lanes of Arm 3				lanes of Arm 4			
	1	2	3	4	1	2	3	1	2	3	4	1	2	3	
Case I	shared-use	E. L.	S.	E. T.	E. T.	E. L.	S.	E. T.	E. L.	S.	E. T.	E. T.	E. L.	S.	E. T.
	conventional	E. L.	E. L.	E. T.	E. T.	E. L.	E. T.	E. T.	E. L.	E. L.	E. T.	E. T.	E. L.	E. T.	E. T.
Case II	shared-use	E. L.	S.	E. T.	E. T.	E. L.	S.	E. T.	E. L.	S.	E. T.	E. T.	E. L.	S.	E. T.
	conventional	E. L.	E. L.	E. T.	E. T.	E. L.	E. T.	E. T.	E. L.	E. L.	E. T.	E. T.	E. L.	E. T.	E. T.
Case III	shared-use	E. L.	S.	E. T.	E. T.	E. L.	S.	E. T.	S.	E. T.	E. T.	E. T.	E. L.	S.	E. T.
	conventional	E. L.	E. L.	E. T.	E. T.	E. L.	E. T.	E. T.	E. L.	E. T.	E. T.	E. T.	E. L.	E. T.	E. T.

[Note] E. L. is short for exclusive left lane; E. T. is short for exclusive through lane; S. is short for shared-use lane.

Fig. 5 plots the effect of length of waiting area on the average delay given the lane assignment. The average delay is high when the waiting area is small because the blockage between the through vehicles and left-turn vehicles dominates. As the length of waiting area increase, the positive effect of shared-use configuration increases and the average delay decreases sharply and levels off if the waiting area is large enough. The trend indicates that the waiting area should not be too small or be unnecessarily large in intersections. Therefore, considering the local geometric layout, the shared-use configuration may not be recommended if the size of an intersection is not able to support the waiting area. If the arrival rate is fixed, the left-turn rate has low effect on the average delay since the results of the optimization will provide more green length and more lanes for the left-turn vehicles. However, if the left-turn arrival rate (or the left-turn proportion) is so high that even with maximum green length and lanes given, left-turn movement maintains high degree of saturation, the curve will rise earlier. Fig. 6 indicates that the optimized average delay of the new configuration increase with the increase of arrival rate. It is similar to the conventional configuration, while the growth rate is expected to be slower than the latter. However, if the arrival rate surpasses the

capacity of intersections, the average delay will increase sharply, which is the result of the high degree of saturation. The result reveals that if the arrival rate in urban intersection is so high that even the shared-use lane combined with the waiting area cannot handle the situation, other methods such as grade separation should be used but not the shared-use method. Therefore, the increase of the performance by using the method is actually limited.

7 Conclusion

The application of the waiting area combined with the shared-use operation is meaningful in urban intersection. Since the shared-use lane can automatically adjust the degree of saturation of through and left-turn vehicles, the potential capacity is hence explored. By providing more capacity for the movement with high degree of saturation, the total performance of the intersection will be improved.

An integrated model is proposed to obtain the optimal design of shared-use lane assignment and signal timing of the configuration. The constraints for the shared-lane assignment are proposed and the capacity of lane groups is recalculated by considering the function of shared-use lane with waiting area. And it's presented the calculation

formula to show the relationship between the capacity of shared-use lane and B , N , M (the formula Eqs. (12)~(16)). Among them, N and M are respectively correlated to the green length of through vehicles in this direction and the green length of left-turn vehicles.

The continuous function relationship between the capacity of lane groups and signal timing is discussed and the average delay as the objective function is presented. In order to get the continuous function relationship of the capacity of shared-use lane on the green time length of the through vehicle, the green time length of the left-turn vehicle, the probability model of N and the through vehicle green duration, M and the left-turn vehicle green duration is shown in Section 3 (especially the Steps 1~5, Eqs. (17)~(22)). A non-linear programming with continuous and binary variables is hence formulated and a feasible directions method together with enumeration of shared-use lane assignment is introduced to obtain the optimal results. The results show that the shared-use lane assignment together with the optimized signal timing in intersections with the waiting area outperforms the conventional configuration.

The sensitivities of the optimized average delay are investigated, which include the length of waiting area and the arrival rates. As the length of waiting area increase, the positive effect of shared-use configuration increases and the average delay decreases sharply and levels off if the waiting area is large enough. However, the trend indicates that the waiting area should not be too small or be unnecessarily large in intersections. And it is also limited by the local geometric layout of intersection, which the size is or not able to support the waiting area. The optimized average delay of the new configuration increase with the increase of arrival rate, but not surpasses the capacity of intersections. Therefore, the increase of the performance by using the method is actually limited.

Further study may focus on the stochastic cases with different arrival processes and empirical performance data. Besides, the adaptability of drivers to the new operation and some specific conditions, such as existence of emergency vehicles and buses, are worth further investigating.

References

- [1] General Administration of Quality and Technical Supervision. National Standards of People's Republic of China: Road Traffic Signs and Markings (GB 5768-1999) [S]. Beijing: Standards Press of China, 1999. (in Chinese)
- [2] General Administration of Quality and Technical Supervision. National Standard Road Traffic Signs and Markings of the People's Republic of China (Part 3): Road Traffic Markings (GB 5768. 3-2009) [S]. Beijing: Standards Press of China, 2009. (in Chinese)
- [3] CHEN Y H, BAI Q W, WEI X Y. Departure processes model for left-turn lanes on waiting area[J]. Journal of Transportation Systems Engineering and Information Technology, 2014, 14(1): 174-179. (in Chinese)
- [4] XUAN Y, DAGANZO C F, CASSIDY M J. Increasing the capacity of signalized intersections with separate left turn phases[J]. Transportation Research Part B: Methodol, 2011, 45:769-781.
- [5] JIANG X G, ZHANG G P, BAI W, et al. Safety evaluation of signalized intersections with left-turn waiting area in China [J]. Accident Analysis & Prevention, 2016, 95(Pt B): 461-469.
- [6] LIU P, WAN J, WANG W, et al. Evaluating the impacts of unconventional outside left-turn lane design on traffic operations at signalized intersections [J]. Transportation Research Record, 2011, 2257:62-70.
- [7] MA W J, LIU Y, ZHAO J, WU N. Increasing the capacity of signalized intersections with left-turn waiting areas [J]. Transportation Research Part A, 2017, 105:181-196.
- [8] SUN D Z. Using micro-simulation VISSIM to study the effectiveness of left-turn waiting area implementation [J]. Applied Mechanics and Materials, 2018, 876:187-191.
- [9] ZHAO X J, HAN Y, YAO J. Effect of waiting area for vehicle emissions [J]. China Water Transport, 2015, 15(12): 160-162. (in Chinese)
- [10] MESSER C J, FAMBRO D B. Effect of signal phasing and length of left-turn bay on capacity [C]// 56th Transportation Research Board Annual Meeting.

- Washington DC: Transportation Research Board, 1977.
- [11] AL-KAISY A F, STEWART J A. New approach for developing warrants of protected left-turn phase at signalized intersections [J]. *Transportation Research Part A*, 2001, 35(6): 561-574.
- [12] YAN X D, RADWAN E. Effect of restricted sight distances on driver behaviors during unprotected left-turn phase at signalized intersections [J]. *Transportation Research Part F Traffic Psychology & Behaviour*, 2007, 10(4): 330-344.
- [13] LIN F B. Saturation flow and capacity of shared permissive left-turn lane [J]. *Journal of Transportation Engineering*, 1992, 118(5): 611-630.
- [14] EASA S M, ALI M Z A. Modified guidelines for left-turn lane geometry at intersections [J]. *Journal of Transportation Engineering*, 2005, 131(9): 677-688.
- [15] ZHANG Yunlong, TONG Jiabin. Modeling left-turn blockage and capacity at signalized intersection with short left-turn bay [J]. *Transportation Research Record: Journal of the Transportation Research Board*, 2008, 2071: 71-76.
- [16] CHANG T H, SUN G Y. Modeling and optimization of an oversaturated signalized network [J]. *Transportation Research Part B Methodological*, 2004, 38(8): 687-707.
- [17] ZHAO L, PENG X S, LI L, et al. A fast signal timing algorithm for individual oversaturated intersections [J]. *IEEE Transactions on Intelligent Transportation Systems*, 2011, 12(1): 280-283.
- [18] ZHU H B, LEI L, DAI S Q. Two-lane traffic simulations with a blockage induced by an accident car [J]. *Physica A Statistical Mechanics & Its Applications*, 2009, 388(14): 2903-2910.
- [19] KRONPRASERT N, KIKUCHI S. Determining lengths of left-turn lanes at signalized intersections under different left-turn signal schemes [J]. *Transportation Research Record: Journal of the Transportation Research Board*, 2010, 2195 (2195): 70-81.
- [20] QI Y G, GUO L, YU L, TENG H L. Estimation of design lengths of left-turn lanes [J]. *Journal of Transportation Engineering*, 2012, 138(3): 274-283.
- [21] IMPROTA G, CANTARELLA G E. Control system design for an individual signalized junction [J]. *Transportation Research Part B Methodological*, 1984, 18(2): 147-167.
- [22] GALLIVAN S, HEYDECKER B. Optimizing the control performance of traffic signals at a single junction [J]. *Transportation Research Part B Methodological*, 1988, 22(5): 357-370.
- [23] SILCOCK J P. Designing signal-controlled junctions for group-based operation [J]. *Transportation Research Part A Policy & Practice*, 1997, 31(2): 157-173.
- [24] FOY M D, BENEKOHAL R F, GOLDBERG D E. Signal timing determination using genetic algorithms [J]. *Transportation Research Record: Journal of the Transportation Research Board*, 1992, 1365: 108-115.
- [25] PARK B. Traffic signal optimization program for oversaturated conditions: Genetic algorithm approach [J]. *Transportation Research Record: Journal of the Transportation Research Board*, 1999, 1683 (1): 133-142.
- [26] CEYLAN H, BELL M G H. Traffic signal timing optimization based on genetic algorithm approach, including drivers' routing [J]. *Transportation Research Part B Methodological*, 2004, 38(4): 329-342.
- [27] MU F F, ZHANG H Z. Signaltiming optimization at single-point intersection based on genetic algorithm [J]. *Journal of University of Shanghai for Science and Technology*, 2015, 37(6): 600-604. (in Chinese)
- [28] LI X, LIU Y, ZHOU J, et al. An optimization model of traffic signal cooperative timing based on improved GA [J]. *Industrial Instrumentation & Automation*, 2017(4): 125-130. (in Chinese)
- [29] MURAT Y S, GEDIZLIOGLU E. A fuzzy logic multi-phased signal control model for isolated junctions [J]. *Transportation Research Part C*, 2005, 13(1): 19-36.
- [30] CHEN C, WONG C K, HEYDECKER B G. Adaptive traffic signal control using approximate dynamic programming [J]. *Transportation Research Part C*, 2009, 17(5): 456-474.
- [31] TEODOROV D, VARADARAJAN V, POPOVIĆ J, et al. Dynamic programming-neural network real-time traffic adaptive signal control algorithm [J]. *Annals of Operations Research*, 2006, 143 (1): 123-131.
- [32] ZHU X N, LONG B. Bi-level programming model of timing optimization for multiple bus priority intersection [J]. *Journal of Traffic and Transportation Engineering*, 2014, 14(1): 103-111. (in Chinese)
- [33] JIANG Y, LI S, SHAMO D E. A platoon-based traffic signal timing algorithm for major-minor intersection types [J]. *Transportation Research Part B Methodological*, 2006, 40(7): 543-562.
- [34] TIAN Z Z, WU N. Probabilistic model for signalized intersection capacity with a short right-turn lane [J]. *Journal of Transportation Engineering*, 2006, 132(3): 205-212.
- [35] HUANG H Q. Application and simulation of signal timing method based on multi-objective joint

- optimization[J]. *Journal of Guangxi University of Science and Technology*, 2018, 29(3): 102-107. (in Chinese)
- [36] SHU L Z, WU J, WANG C. Urban traffic signal control based on deep reinforcement learning [J]. *Journal of Computer Applications*, 2019, 39(5): 1495-1499. (in Chinese)
- [37] LAM W H K, POON A C K, MUNG G K S. Integrated model for lane-use and signal-phase designs [J]. *Journal of Transportation Engineering*, 1997, 123(2):114-122.
- [38] WONG C K, WONG S C. Lane-based optimization of signal timings for isolated junctions[J]. *Transportation Research Part B Methodological*, 2003, 37(1): 63-84.
- [39] WONG C K, HEYDECKER B G. Optimal allocation of turns to lanes at an isolated signal-controlled junction [J]. *Transportation Research Part B Methodological*, 2011, 45(4): 667-681.
- [40] JANSON B N, FINOCHIO M R. Estimation of de facto left-turn lanes at signalized intersections [C]// *Traffic Flow Theory and Highway Capacity*. Washington DC: Transportation Research Board, 2001: 100-105.
- [41] BONNESON J A. Lane volume and saturation flow rate for multilane intersection approach[J]. *Journal of Transportation Engineering*, 1998, 124(3): 240-245.
- [42] ZHOU Y P, ZHUANG H B. Traffic performance in signalized intersection with shared lane and left-turn waiting area established[J]. *Journal of Transportation Engineering*, 2012, 138(7): 852-862.
- [43] WEBSTER F V. Traffic signal settings [C]// *Road Research Technical Paper No. 39*. London: Road Research Laboratory, 1958.